XPS Study of the Effect of Aluminium on the Atmospheric Corrosion of the AZ31 Magnesium Alloy

S. Feliu Jr,[a] M.C. Merino,[b,*] R. Arrabal,[c] A. E. Coy,[c] E. Matykina[c]

[a]*Centro Nacional de Investigaciones Metalúrgicas CSIC, Avda. Gregorio del Amo 8, 28040 Madrid, Spain*

[b]*Departamento de Ciencia de Materiales, Facultad de Química, Universidad Complutense, 28040, Madrid, Spain*

[c]*Corrosion and protection Centre, School of Materials, The University of Manchester, P.O. Box 88, Sackville Street, Manchester, M60 1QD, United Kingdom*

[*]Corresponding author. Tel: +34 1 3944348; Fax: +34 1 3944357

E-mail: cmerinoc@quim.ucm.es

ABSTRACT: The surface characteristics and corrosion behaviour of the AZ31 magnesium alloy exposed to a high relative humidity (RH) atmosphere were investigated. During the first 15 days of humidity test at 98% RH and 50ºC, a significant increase of magnesium carbonate and a decrease of magnesium oxide were detected on the surface film by X-Ray photoelectron spectroscopy (XPS); after this stage, increased exposure times did not produce substantial changes on the relative amounts of these compounds. The surface film of commercially pure magnesium, also examined for comparison purposes, revealed more magnesium carbonate and less magnesium oxide compared with the AZ31 alloy. Unlike the AZ31 alloy, the surface of pure Mg disclosed almost complete substitution of MgO by magnesium carbonate after 30 days of exposure time. Mass gain values of tested specimens and scanning electron microscope characterization of corroded surfaces indicated lower corrosion susceptibility of the AZ31 alloy compared with the commercially pure Mg, suggesting superior chemical stability of the oxide/hydroxide film formed over the magnesium-aluminium alloy surface. XPS and EDX analysis did not revealed any substantial enrichment of aluminium in the corrosion products film on the AZ31 alloy after 30 days of testing.

KEYWORDS: Magnesium/aluminium alloys; XPS; Magnesium carbonate; Magnesium oxide.

1. INTRODUCTION

Corrosion properties of magnesium alloys understandably become of great interest because of their wide use in many engineering applications [1]. The stability of the magnesium depends mainly of the protective ability of the oxide film that spontaneously cover its surface due to the great affinity of this metal to oxygen [1, 2, 3]. However, the corrosion resistance is limited for exposure to the atmosphere or to aqueous solutions because the oxide reacts with water and forms poorly protective hydroxide layer[1, 2, 3, 4, 5]. The aluminium, similar to magnesium, has an strong tendency to react with oxygen. The positive effect of aluminium as alloying element on corrosion resistance of magnesium has been investigated in many experimental conditions, e.g. exposure to dry oxygen,[2, 4] normal atmosphere,[3,6, 7] high humidity atmospheres,[8, 9, 10, 11, 12] immersion in distilled water,[13] saline solutions,[14, 15, 16, 17, 18] etc. It is well known that addition of Al to Mg based alloys causes the formation of aluminium oxide film or mixtures of Mg and Al oxides, with increased stability of the exposed surface compared with pure Mg.[16, 17, 19, 20] . Thermodinamical estimations allows to predict which alloy constituent (Mg or Al) will be preferentially oxidized upon oxidation of a Mg-Al substrate. The result is function, between other factors of the Al concentration at the bare alloy surface [21]. In a dry atmosphere, the Mg and Al get incorporated during the initial, very fast, oxidation regime, whereas Mg gets preferentially oxidized during the succeeding stage of oxide film growth [21] . On the other hand, contact with humidity leads to an oxide layer containing relatively larger amounts of hydroxyl or hydroxide species, in which composition the alloying Al may participate considerably [4, 5, 22]. En general, the mechanisms of improvement due to Al additions to Mg-based alloys es todavía insuficientemente conocido y merece un mayor estudio.

A great deal of attention has been paid to the role of the β-phase on the corrosion mechanism of magnesium/aluminium alloys. A generally accepted idea is that this phase acts as an effective cathode and/or barrier against corrosion, depending on its size and distribution.[11, 16, 23, 24] Therefore, as well as aluminium content, the alloy microstructure plays a key role in determining the corrosion susceptibility of magnesium-aluminium alloys, especially for high aluminium alloys such as the well-known AZ91 alloy (~ 9 wt.% Al).[4, 11, 12, 15, 24, 25]

The present study concerns the atmospheric corrosion behaviour of the AZ31 alloy. Since it is a single-phase alloy with 3 wt%. aluminium in solid solution, the effect of this element on the corrosion performance of the alloy can hardly be explained in terms of microstructural changes when compared with commercially pure Mg. Previous study of the AZ31 alloy under the same environmental conditions (98% RH; 50ºC) revealed an important reduction of corrosion susceptibility compared with pure Mg[26] . The properties of the oxide/hydroxide film formed on the surface often determine the atmospheric corrosion behaviour of the magnesium alloy. Assuming the hypothesis that the performance of the alloy relies upon the chemistry of its oxide film, its characterization is of considerable importance. In the present study, XPS is used in order to characterize the surface film of the AZ31 alloy exposed to a high humidity environment. The findings revealed compositional changes in the oxide film during the humidity test, which provided further knowledge about the different behaviour of the AZ31 alloy with respect to pure Mg.

2. EXPERIMENTAL PROCEDURE

2.1. Test Materials

Table 1 shows the chemical composition of the AZ31 magnesium alloy. Unalloyed Mg was used as a reference material. Pure Mg and AZ31 alloy were fabricated in wrought condition by Magnesium Elektron Ltd.

2.2 Gravimetric tests

Specimens of working area of ~ 15 cm^2 were rinsed with deionized water, dried in warm air and weighed prior to the gravimetric measurements. The accelerated atmospheric tests consisted of 24 h cycles performed in a saturated water vapour at 98% RH and 50ºC during 28 days simulated by a humidity condensation cabinet CCK 300 (Dycometal). The samples were suspended vertically above the water-covered cabinet floor. The temperature and the humidity were verified using a digital thermometer and hygrometer. At the end of the tests, the specimens were rinsed with deionized water, dried in warm air and weighed again. Corrosion rate was calculated from the mass gain per unit of surface area, calculated from the expression $(M_f - M_i)/A$, where M_f is the final mass, M_i is the initial mass and A is the exposed surface area. In all cases, the tests were performed twice to ensure the reproducibility of the results. En estos ensayos, se han encontrado desviaciones máximas del orden del 10%.

2.3 SEM Characterization

The surface of specimens exposed to a high relative humidity environment was examined by scanning electron microscopy (SEM) using a JEOL JSM-6400 microscope equipped with Oxford Link energy dispersive X-ray (EDX) microanalysis hardware.

2.4 Surface analysis

Photoelectron spectra were acquired with a Fisons MT500 spectrometer equipped with a hemispherical electron analyser (CLAM 2) and a non-momochromatic magnesium Kα X-ray source operated at 300 W. The samples were mechanically fixed on small flat discs supported on an XYZ manipulator placed in the analysis chamber. The residual pressure in this ion-pumped analysis chamber was maintained below 10^{-8} Torr during data acquisition. The spectra were collected for 20-90 min, depending on the peak intensities at a pass energy of 20 eV, which is typical of high-resolution conditions. The intensities were estimated by calculating the area under each peak after smoothing and substraction of the S-shaped background and fitting the experimental curve to a mix of Lorentzian and Gaussian lines of variable proportion. Although sample charging was observed, accurate binding energies (BE) could be determined by referencing to the adventitious C1s peak at 285.0 eV. Atomic ratios were computed from peak intensity ratios and reported atomic sensitivity factors.[27]. The sampled areas were 1 x 1 mm^2. The energy resolution is about 0.8 eV.

Bombardment was performed using an EXO5 ion gun incorporated into the equipment, provided with a scanning unit to track the beam, operating at a voltage of 5 kV, an intensity of 10 mA and a pressure of $1x10^{-7}$ Torr. The sample current was 1 μA during bombardment. According to information in the literature[28, 29] this specimen current is equivalent to a sputtering rate of about 2 Å/min. Previous author's results on interstitial-

free (IF) steels disclosed a sputtering rate of 1.5 Å/min, suggesting similar sputtering rate for the bombardment conditions and the spectrometer used in this study.[30] Prior to recording of XPS spectra, the specimens were sputtered for 10 minutes in order to remove surface contaminants (equivalent to about 2 nm of thinning).

The XPS results for the pure Mg and AZ31 alloy are the average of the data obtained in duplicate after cleaning the specimens with distilled water

3. RESULTS AND DISCUSSION

3.1. Initial stage (1-15 days of exposure to the humidity test)

Table 2 shows the elemental composition of the sputter-cleaned surfaces of pure Mg and AZ31 alloy obtained by XPS before and during the humidity test. The surface of as-received specimens revealed high carbon content, indicating that the cleaning process did not completely remove impurities from the surface, such as oils used during the storage and transportation of these materials. After one day in the humidity chamber, an important reduction in the carbon content and a relative increase of oxygen and magnesium were detected. These changes may to be related with the replacement of the initial metallic magnesium surface by magnesium corrosion products which are less enriched in C-C/C-H groups. Extended exposure times did not produce significant changes in the atomic contents.

For the unexposed surface of the AZ31 alloy, the Al/(Al+Mg) atomic ratio was ~ 0.14, which is significantly higher than the 3 wt.% of aluminium present in the bulk alloy. Se podría pensar que este enriquecimiento se haya producido por una segregación de Al durante the manufacturing stages when the material is exposed to high temperatures, or during storage of specimen in normal room temperature prior to the experiments. Sin

embargo, el hecho de que no se revele la presencia de Al before surface cleaning with Ar^+ ion (trabajo en preparación) parece descartar esta posibilidad. Recientemente, it has been shown that a strong Al enrichment develops in the subsurface region of sputter-cleaned Mg alloys due to preferential sputtering of Mg in combination with the simultaneous bombardment-enhanced Gibbsian segregation of Mg to the free surface[21]. Por lo tanto, cabe la posibilidad de que el enriquecimiento observado en este trabajo se deba simplemente a este último fenómeno. Nevertheless, the Al/(Al+Mg) ratio decreased with the exposure time and was slightly higher than the theoretical value after 15 days in the humidity chamber (Table 2), seguramente por una progresiva acumulación en la superficie de la probeta de productos de corrosión formados durante el ensayo.

Due to strong overlap between the second bulk plasmon of the metallic Mg2p peak and the Al2p peak observed in our measurements. we have measured the Al2s peak instead of the Al2p peak [31]. The high resolution Al2s spectra for the unexposed surface of the AZ31 alloy revealed a single component at 120.5 eV typical of aluminium in the form of Al_2O_3 (Figure 1)[32]. In order to interpret the XPS spectrum of the magnesium and AZ31 alloy, tabulated data[1,2,3,33] (Table 3) were used for the XPS spectroscopy peak position related to Mg and Mg compounds.

Mg2p XPS high resolution spectra of pure Mg and AZ31 alloy are compared in Figure 2. As-received pure Mg revealed the highest intensity peak at a binding energy of 49.8 eV, which is associated with the presence of magnesium in the elemental state (Figure 2a). At 51.8 eV a peak of lower intensity was also found, related to magnesium in the form of Mg^{2+}.[33] After one day the absence of Mg° is noticeable, indicating a significant growth of the oxide film on pure Mg exposed to the high humidity environment (Figure

2b). For increased exposure times, XPS spectra are broad and centered between 51.5 and 51.9 eV, indicating seguramente the co-existence of Mg oxide, Mg hydroxide or Mg carbonate. Likewise, no significant differences were observed in the Mg2p spectra of the AZ31 alloy for exposure times longer than one day.

Figure 3 compares the evolution of the C1s high resolution XPS spectra of pure Mg and AZ31 alloy exposed to the humid environment. For the sputter-cleaned unexposed surfaces, XPS spectra can be fitted with three components (Figures 3a and 3e). The first and more intense peak, located at 285.0 eV, is associated with the presence of C-C/C-H groups (adventitious hydrocarbon contamination).[30] At 286.5 and 288.0 eV, the second and third components of lower intensity, related to C-O and C=O groups, respectively, have practically disappeared after one day in the humid environment (Figures 3b and 3f). As a consequence of the humid atmosphere, the component at higher binding energies shifted 1.5-2 eV and gained intensity with increasing exposure time. According to the literature,[2, 34] this component at 290.3-290.8 eV corresponds to carbonate, suggesting a significant amount of magnesium carbonate over the surface of tested specimens (Figures 3b-3h).

High resolution O1s spectra of pure Mg and AZ31 materials can be fitted with three components (Figures 4a and 4e). The first one is situated at approximately 531.0 eV, and normally is interpreted as oxygen in the form of magnesium oxide, MgO.[2, 4, 33] The quantitative ratio between Mg2p and the O1s component at 531.0 eV is between 0.8-1.2 which is fairly consistent with the theoretical ratio 1.00 for MgO (Table 2)[33]. The second binding energy peak at 533.0 eV, can possibly be associated with OH^- and C=O groups. And, at higher binding energies (534.0 eV), a C-O component (demonstrated by

the C1s peak). It is interesting to note that prior to recording of XPS spectra, the specimens were sputtered for 10 minutes in order to remove surface contaminants. Due to this treatment the surface of the specimen have been altered from $Mg(OH)_2$ to MgO[35] . Also the ten minutes of AIB (equivalent to about 2 nm of thinning) have been probably sufficient to eliminate the signal of water and OH^- adsorbed groups in the outermost surface. After one day of exposure, the component at 534.0 eV disappeared, the MgO component in pure Mg diminished compared with the AZ31 alloy and the peak at 533.2-533.4 eV, attributed to the presence of $MgCO_3$ and/or $Mg(OH)_2$,[34] became more prominent with the exposure time.

Figure 5 compares the evolution of carbonate and/or hydroxide atomic percent on the surface of pure Mg and the AZ31 alloy exposed to humid air. The values presented in Figure 5a were obtained from the fitting of the $CO_3^=$ component of the C1s peak (Fig.3), while Figure 5b data was determined from the area of the second component in the O1s spectra. Similar trends are observed in Figures 5a and 5b and an approximately linear relation is obtained from comparison of the atomic percents in Figure 5c. This supports the assignment of the high energy component of the O1s peak mainly to the magnesium carbonate and suggests the formation of magnesium carbonates over the surfaces exposed to the humid atmosphere. In addition, O/Mg, O/C and Mg/C atomic ratios rapidly evolved to 3, 3 and 1, respectively, which are expected values for stoichiometric magnesium carbonates (Table 2).

Evolution of MgO content with the exposure time, obtained from the fitting of the O1s peak, is presented in Figure 6. A reduction on the atomic percents of MgO for both tested materials was revealed during the first 15 days in the humid environment.

3.2. Second stage (15-30 days of exposure to the humidity test)

Following the previous trend observed during the first 15 days of humidity test, the MgO atomic percent on the surface of pure Mg decreased and almost disappeared after 30 days of exposure to the humid environment. The surface of the AZ31 alloy revealed different behaviour; the amount of MgO remained practically constant between 15 and 30 days (Figure 6). The carbonate content slightly increased for pure Mg and remained constant for the AZ31 alloy (Figure 5a).

The presented XPS results are consistent with the atmospheric corrosion behaviour of the AZ31 alloy and pure Mg. Considering the mass gain values of studied materials exposed to 98% RH at 50°C, which are associated with the oxidation, hydration and carbonation reactions taking place at the exposed surfaces, 3 wt.% of aluminium in the AZ31 alloy has reduced the corrosion degradation up to about 35% (Table 4).

Scanning electron micrographs of pure AZ31alloy (Fig.8a) and pure magnesium (Fig. 8b) after 30 days of exposure in the humidity test confirmed the above results. Thus, for pure Mg, a greater area of the surface was covered by corrosion products (Fig. 8b) compared with the AZ31 alloy (Fig 8a), where corrosion products where less abundant and slightly whiter.

3.3 Aluminium effect

In case of the AZ31 magnesium alloy, 3 wt.% aluminium in the composition of bulk alloy is insufficient to facilitate the precipitation of the β-phase ($Mg_{17}Al_{12}$). Due to the

presence of manganese (0.25 wt.%), some Al-Mn inclusions were observed in the microstructure of this alloy (Figure 7). Although these inclusions are detrimental for the corrosion susceptibility of magnesium-aluminium alloys immersed in aqueous solutions, their effect on the atmospheric corrosion behaviour is almost insignificant, since the electrolyte layer in atmospheric environments is thin and the driving force between the Al-Mn inclusions and the surrounding material is not strong enough for the initiation of a corrosion attack in the vicinity of these particles.[35] Thus, aluminium effect on the atmospheric corrosion behaviour of this alloy compared with pure Mg can not be explained in terms of microstructural changes. On the other hand, aluminium may significantly contribute to corrosion resistance by improving the properties of the surface film.[6, 9, 12, 19]

The morphology and structure of the oxide film formed on Mg-Al alloys have been investigated in detail by Nordlien et al.[7, 13, 19, 20] Similarly to pure Mg, the initially air-formed film is amorphous and dense; the oxide formed in water exhibits a three-layered structure consisting of a hydrated inner layer, a dense intermediate layer similar in structure to the air formed film, and a top layer with platelet-like morphology.[19] With increase of Al content in magnesium alloy, all layers become dehydrated and enriched in aluminium oxide. The beneficial effect of these changes are evident in the corrosion behaviour of the AZ31 alloy.[19,20] According to Lindstrom et al,[10] the significant improvement in corrosion resistance of Mg-Al alloys may be attributed mainly to the alumina component of the inner layer becoming the dominant factor in determining the passivity of the surface.

In a carbon dioxide (CO_2) containing atmosphere, when a thin electrolyte layer is present on the metal surface, CO_2 readily diffuses to the film surface and tends to form magnesium carbonate. In addition, it is generally accepted that CO_2 lowers the pH in the areas of the surface that are alkaline due to the cathodic reaction, resulting in a decreased solubility of aluminium and stabilization of the Al-containing surface film.[11, 22]

Analysis of the findings of the present study confirmed a higher amount of MgO on the surface of unexposed AZ31 alloy compared with pure Mg (Figure 6). Also, a significant increase in the intensity of the $Mg(OH)_2$/C=O component observed in the unexposed surface of pure Mg (Fig. 4a) compared with that of the AZ31 alloy (Fig. 4e). The fitting of the C1s spectra (Fig. 3a and 3e) suggests that the atomic percents of C=O groups are quite similar for both materials (data not presented here), and therefore, the amount of $Mg(OH)_2$ on the surface of pure Mg (Fig. 4a) is higher than the one for the AZ31 alloy (Fig. 4e). These results suggest that the presence of aluminium as alloying element in single-phase magnesium alloys favours the formation of MgO rather than $Mg(OH)_2$ on the surface film. EDX analysis of the surface of the AZ31 alloy after 30 days at 98% RH and 50°C (Fig. 8a points 5 and 6) corroborates the idea of a significant amount of MgO on the surface film at the end of the experiment (Table 5). In addition, XPS spectra did not revealed any significant variations in the amount of MgO in the surface film of the AZ31 alloy, which is completely opposite to what is observed for pure Mg (Fig. 6). The reduction of the amount of $Mg(OH)_2$ and its substitution by $MgCO_3$ on the surface of both materials (Fig. 5) could be interpreted as a result of the localized corroded areas rich in $Mg(OH)_2$ acting as favourable places for the formation and accumulation of magnesium carbonates.

After 30 days in the humidity chamber, the important role of aluminium on the mechanism of atmospheric corrosion of the AZ31 alloy becomes clear. Thus, Figure 8b shows the surface of pure Mg completely covered with a rather uniform corrosion film, in which may predominate magnesium carbonates (Table 5). On the other hand, corrosion layer on the surface of the AZ31 alloy is uneven (Fig. 8a) with some areas chiefly covered by MgO and the remaining places covered with thicker corrosion products containing $MgCO_3$ (Table 5). These results are in agreement with XPS observations, where, after 30 days, O1s spectrum obtained for the pure Mg (Fig. 4d) showed $MgCO_3$ as the main component accompanied by a small amount of MgO, and the corresponding O1s spectrum obtained for the AZ31 alloy (Fig. 4h) revealed a significant fraction of MgO along with $MgCO_3$.

The Al/(Mg+Al)x100 ratio for the surface film of the AZ31 alloy is slightly higher than the aluminium content in the bulk metal composition after 15-30 days (Table 2). Therefore, according to XPS results there is no aluminium enrichment on the outer surface of the corrosion products (~20 Å). Likewise, EDX analysis with much higher signal penetration (~ 1 μm), did not detect higher aluminium content in the corrosion film formed on the AZ31 alloy compared with the bulk metal composition (Fig. 8a). It is feasible to suppose that aluminium enrichment responsible of the higher corrosion resistance has occurred in a thin oxide layer, presumably near the metal/oxide interface.

In the literature, there are diverse results regarding the possibility of aluminium enrichment in corrosion products film formed on magnesium-aluminium alloys. For instance, XPS analysis of the composition of the film on the AZ91 alloy after immersion in 1N NaCl at pH 11 did not reveal any significant aluminium

enrichment.[16] Neither is clear the aluminium incorporation into the corrosion film layer on the AZ91 alloy during exposure to humid air with NaCl, which was shown to be mainly composed by magnesite (at 75% RH), hydromagnesite and brucite (at 95% RH).[12] However, significant aluminium enrichment in the oxide film covering the AZ91 alloy at the initial stages of atmospheric corrosion has been observed at room temperature.[11] An enrichment in aluminium and magnesium oxides was found after immersion of the AZ91 alloy in distilled water and the formation of aluminium and magnesium hydroxides after exposure to salt spray.[15] All the above results suggest that the aluminium enrichment on the surface of magnesium-aluminium alloys is a phenomenon greatly influenced by the testing conditions.

4. CONCLUSIONS

1. XPS analysis has been shown as a useful instrument for the examination of protection mechanisms of the AZ31 magnesium alloy exposed to high relative humidity.

2. For commercially pure Mg, the detected CO_3^{2-} atomic percent increases, whereas the amount of MgO continuously decreases during the test. This result suggests that the magnesium oxide readily reacts with the CO_2 from the air forming magnesium carbonate.

3. Although the surface film of the AZ31 alloy containing aluminium oxides/hydroxides slightly inhibits the magnesium carbonate formation, it does not prevent its formation in significant amounts.

4. After exposure for 15 days, XPS analysis of the AZ31 alloy surface disclosed appreciable amounts of oxides and carbonate, which did not significantly change after 30 days of the humidity test, suggesting stabilization of the surface composition due to the presence of aluminium.

5. The reduced corrosion rate of the AZ31 alloy compared with pure Mg during the humidity test is likely to be due to a higher chemical stability of the oxide film formed on the AZ31 alloy. However, XPS and EDX analysis did not reveal any significant enrichment of aluminium oxide in the corrosion products film, which suggests that aluminium enrichment only affects a very thin layer of the oxide film, presumably near the metal/oxide interface.

Acknowledgements. The authors wish to thank the Community of Madrid and MCYT for the financial support to carry out this investigation through the program ESTRUMAT_CM (reference MAT/77) and (MAT2006-13179-C02-02).

REFERENCES

1. M. Santamaria, F. Di Quarto, S. Zanna, P. Marcus, *Electrochim. Acta.* **2007**; 53, 1314.
2. V. Fourier, P. Marcus, I. Olefjord, *Surf. Interface Anal.* **2002**; 34, 494.
3. C. Fotea, J. Callaway, M. R. Alexander, *Surf. Interface Anal.* **2006**; 38, 1363.
4. J. Kim, K. C. Wong, P. C. Wong, S. A. Kunlich, J. B. Metson, K. A. R. Mitchell, *Appl. Surf. Sci.* **2007**; 253, 4197.
5. C. Chen, S.J. Splinter, T. Do, N.S. McIntyre, *Surf. Sci*, 1997; 382, L652.
6. N. S. McIntyre, C. Chen, *Corros. Sci.* **1998**; 40, 1679.
7. J. H. Nordlien, S. Ono, N. Masuko, K. Nisancioglu, *Corros. Sci.* **1997**; 39, 1397.
8. S. J. Splinter, N. S. McIntyre, *Surf. Sci.* **1994**; 314, 157.
9. R. Lindström, J. E. Svenson, L. -G. Johansson, *J. Electrochem. Soc.* **2002**; 149, B103.
10. R. Lindström, L. -G. Johansson, G. E. Thompson, P. Skeldon, J. -E. Svensson, *Corros. Sci.* **2004**; 46, 1141.
11. M. Jönsson, D. Persson, R. Gubner, *J. Electrochem. Soc.* **2007**; 154, C684.
12. M. Jönsson, D. Persson, D. Thierry, *Corros. Sci.* **2007**; 49, 1540.
13. J. H. Nordlien, S. Ono, N. Masuko, K. Nisancioglu, *J. Electrochem. Soc.* **1995**; 142, 3320.
14. G. Baril, N. Pebere, *Corros. Sci.* **2001**; 43, 471.
15. G. Ballerini, U. Bardi, R. Bignucolo, G. Ceraolo, *Corros. Sci.* **2005**; 47, 2173.
16. G. Song, A. Atrens, X. Wu, B. Zhang, *Corros. Sci.* **1998**; 40, 1769.
17. A. Pardo, M. C. Merino, A. E. Coy, R. Arrabal, F. Viejo, E. Matykina, *Corros. Sci.* **2008**; 50, 823.
18. G. Song, A. Atrens, D. Stjohn, J. Naim, Y. Li. *Corros. Sci.* **1997**; 39, 855.

19. J. H. Nordlien, K. Nisancioglu, S. Ono, N. Masuko, *J. Electrochem. Soc.* **1996**; 143, 2564.

20. J. H. Nordlien, K. Nisancioglu, S. Ono, N. Masuko, *J. Electrochem. Soc.* **1997**; 144, 461.

21. L.P.H. Jeurgens, M.S. Vinodh, E.J. Mittemeijer, *Acta Mater.* in press.

22. G. Song, A. Atrens, M. Dargusch, *Corros. Sci.* **1999** ; 41, 249.

23. O. Lunder, J. E. Lein, T. Kr. Aune, K. Nisancioglu, *Corrosion* **1989**; 45, 741.

24. G. Song, A. Atrens, M. Dargusch, *Corros. Sci.* **1999**; 41, 249.

25. R. Lindström, L. G. Johansson, J.-E. Svensson, *Mater. Corros.* **2003**; 54, 587.

26. S. Feliu Jr, A. Pardo, M.C. Merino, A.E. Coy, F. Viejo, R.Arrabal, submitted to *Appl. Surf. Sci.*

27. C. D. Wagner, L. E. Davis, M. V. Zeller, J. A. Taylor, R. H. Raymond, L. Gale. *Surf. Interface. Anal.* **1981**; 3, 211.

28. E. McCafferty, M. K. Bernett, J. S. Murday, *Corros. Sci.* **1982**; 28, 559.

29. P. T. Moseley, G. Tappin, J. C. Riviere, *Corros. Sci.* **1982**; 22, 69.

30. S. Feliu (Jr), M. L. Perez-Revenga, *Metall. Mater. Trans.* A, **2004**; 35A, 2039.

31. L.P.H. Jeurgens, M.S. Vinodh, E.J. Mittemajier *Appl. Surf. Sci.* **2006**; 253, 627

32. J. Weiβ, H. J. Miel, R. A. Fischer, C. Wöll, *Chem. Vap. Deposition*, **1998**; 4, 17.

33. H. B. Yao, Y. Li, A. T. S. Wee, *Appl. Surf. Sci.* **2000**; 158, 112-119

34. N.C. Hosking, M. A. Ström, P. H. Shipway, C. D. Rudd, *Corros. Sci.* **2007**; 49, 3699.

35. K.Asami, S. Ono, *J. Electrochem. Soc.* **2000;** 147, 1408.

36. R. Lindström, Ph.D. thesis, Göteborg University, Göteborg, **2003**.

FIGURE CAPTIONS

Table 1. Chemical composition of the samples (weight percent).

Table 2. Chemical composition of the surface of pure Mg and AZ31 alloy unexposed and during the humidity test.

Table 3. Table 3. Reference[1,2,3,33] and measured binding energy(eV) values of Mg and Mg compounds .

Table 4. Mass gain values for samples of pure Mg and AZ31 alloys exposed at 98% RH and 50ºC.

Table 5. EDX analyses of corroded surfaces of AZ31 alloy and pure Mg specimens.

Figure 1. High resolution Al2s spectra obtained on the unexposed AZ31 alloy.

Figure 2. High resolution Mg2p spectra obtained on the unexposed pure Mg and AZ31 alloy and their evolution with the time of exposure.

Figure 3. High resolution C1s spectra obtained on the unexposed pure Mg and AZ31 alloy and their evolution with the time of exposure.

Figure 4. High resolution O1s spectra obtained on the unexposed pure Mg and AZ31 alloy and their evolution with the time of exposure.

Figure 5. (a) Evolution of carbonate atomic percent obtained from the fitting of the C1s Peak; (b) atomic percent of carbonate and/or hydroxide from the O1s; (c) Correlation between atomic percents calculated from C1s and O1s peaks.

Figure 6. Evolution with exposure time of MgO atomic percent obtained from the fitting of the O1s peak (Figure 4).

Figure 7. Scanning electron micrograph of the AZ31 alloy.

Figure 8. Plan views scanning electron micrographs of the (a) AZ31 alloy and (b) pure Mg after 30 days of humidity test.

Table 1

Material	Elements (wt.%)									
	Al	Zn	Mn	Si	Cu	Fe	Ni	Ca	Zr	Others
Mg	0.006	0.014	0.03	0.019	0.001	0.004	<0.001			
AZ31	3.1	0.73	0.25	0.02	<0.001	0.005	<0.001	<0.01	<0.001	<0.30

Table 2

Material	t(days)	%C	%O	%Mg	%Al	Al/(Mg+Al)x100	LBE O1s component/Mg atomic ratio
Pure Mg	0	53 (±5)	35(±3)	12(±2)	0(±0)	0	1.0
	1	24 (±3)	56(±2)	20(±1)	0(±0)	0	0.9
	15	18 (±4)	61(±2)	21(±2)	0(±0)	0	0.8
	30	21 (±5)	62(±2)	17(±3)	0(±0)	0	0.3
AZ31	0	48 (±4)	37(±2)	12(±2)	2(±1)	14	2
	1	25(±4)	52(±2)	21(±1)	2(±1)	9	1.2
	15	22(±3)	55(±1)	22(±1)	1(±1)	4	0.8
	30	16(±5)	61(±2)	22(±2)	1(±1)	4	1.0

Table 3. Reference[1,2,3,33] and measured binding energy(eV) values of Mg and Mg compounds

main peaks.

Peak	Mg metal	MgO	$Mg(OH)_2$	CO_3Mg
Reference values				
Mg 2p	50.2[1] 49.8[2] 49.6 [3] 49.5[33]	51.5[1] 50.8[2] 50.6[33]	51.5[1] 50.8[2] 51.4[3]	52.2[1] 51.9[2]
C 1s				290.6[1] 290.5[2] 290.1[3]
O 1s		531.7[1] 531.0[2] 530.4 [3] 531.0 [33]	532.5[1] 532.4 [2] 532.4[3] 533.2[33]	533.2[1] 532.9[2] 533.4 [3] 534.7[33]
Measured values				
Mg2p	49.8	51.5-51.9	51.5-51.9	51.5-51.9
C1s				290.3-290.8
O1s		531.0	533.0	533.2-533.4

[1] V. Fourier, P. Marcus, I. Olefjord, *Surf. Interface Anal.* **2002**; 34, 494.
[3] H. B. Yao, Y. Li, A. T. S. Wee, *Appl. Surf. Sci.* **2000**; 158, 112-119.
[5] C. Fotea, J. Callaway, M. R. Alexander, *Surf. Interface Anal.* **2006**; 38, 1363.
[7] M. Santamaría, F. Di Quarto, S. Zanna and P. Marcus, *Electrochim. Acta*. **2007**:53, 1314.

Table 4

Exposure time (days)	Mass gain (mg/cm^2)	
	Pure Mg	AZ31
4	0.102	0.006
14	0.354	0.219
20	0.396	0.279
28	0.499	0.332

Table 5. EDX analyses of corroded surfaces of AZ31 alloy and pure Mg specimens.

AZ31 alloy (Fig. 8a, average values of points 1-4 and 5,6)					
Points	%O	%Mg	%Al	O/Mg ratio	Assumed compound
1, 2, 3, 4	81	18	0.3	4.5	$MgCO_3$
5, 6	59	40	0.5	1.5	MgO

Pure Mg (Fig. 8b)				
%O	%Mg	%Al	O/Mg ratio	Assumed compound
84	15	0	5.6	$MgCO_3$

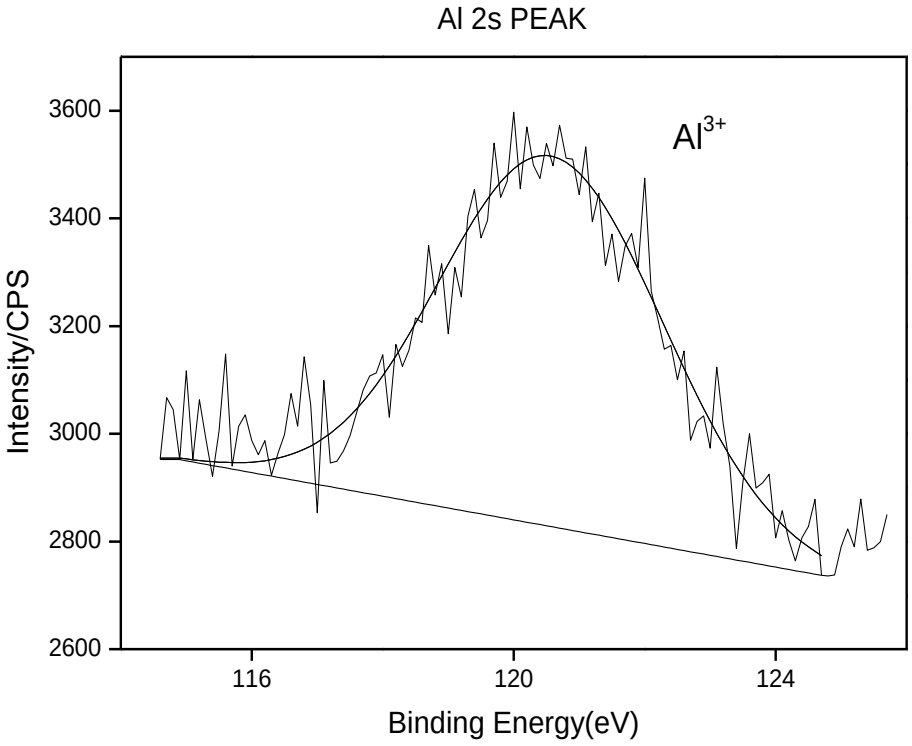
Al 2s PEAK
Al3+
Intensity/CPS
3600
3400
3200
3000
2800
2600
116
120
124
Binding Energy(eV)

Figure 1

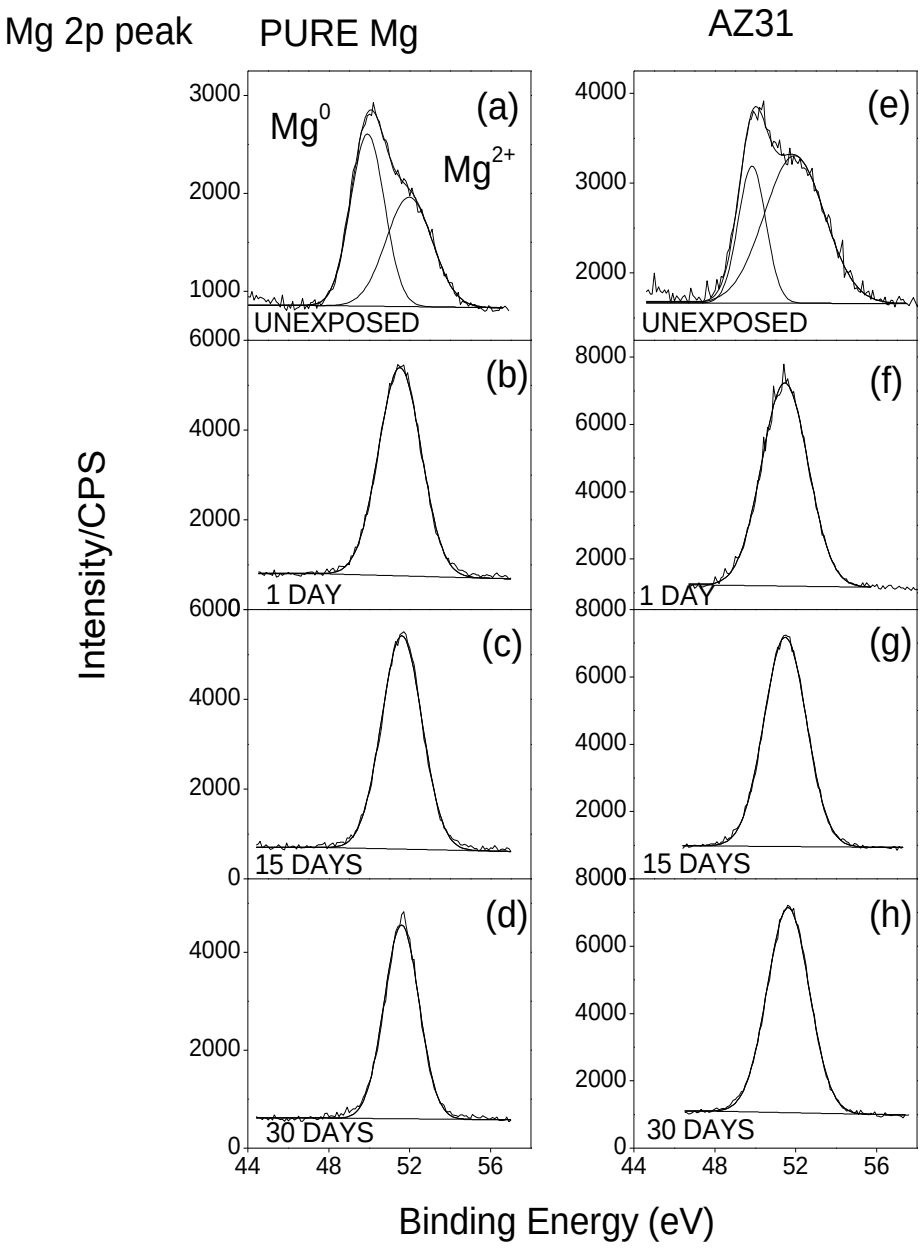
Mg 2p peak
PURE Mg
AZ31
Mg0
Mg2+
(a)
(b)
(c)
(d)
(e)
(f)
(g)
(h)
UNEXPOSED
1 DAY
15 DAYS
30 DAYS
Intensity/CPS
Binding Energy (eV)

Figure 2

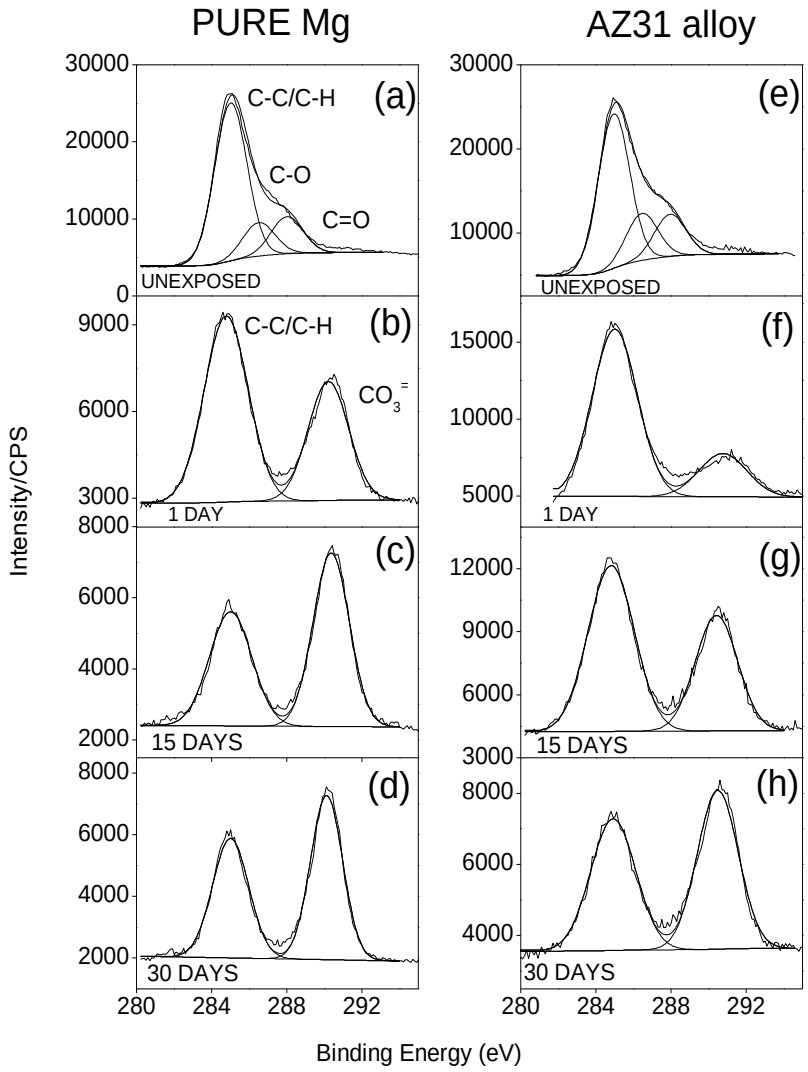
C1s peak
PURE Mg
AZ31 alloy
(a)
C-C/C-H
C-O
C=O
UNEXPOSED
(b)
C-C/C-H
$CO_3^=$
1 DAY
(c)
15 DAYS
(d)
30 DAYS
(e)
UNEXPOSED
(f)
1 DAY
(g)
15 DAYS
(h)
30 DAYS
Intensity/CPS
Binding Energy (eV)

Figure 3

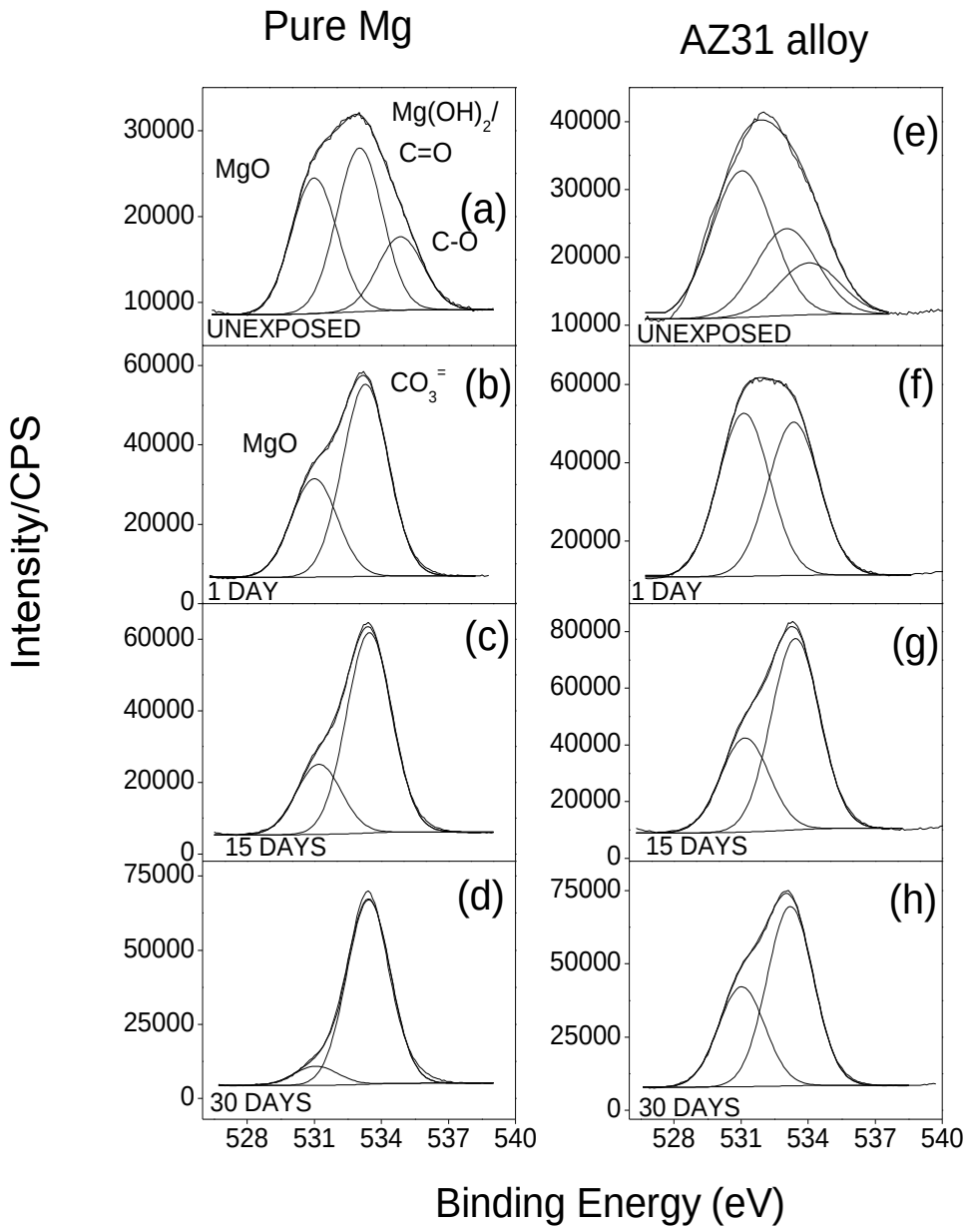
O1s peak
Pure Mg
AZ31 alloy
Intensity/CPS
Binding Energy (eV)
Mg(OH)2/
C=O
MgO
C-O
(a)
UNEXPOSED
CO3=
(b)
MgO
1 DAY
(c)
15 DAYS
(d)
30 DAYS
(e)
UNEXPOSED
(f)
1 DAY
(g)
15 DAYS
(h)
30 DAYS
528
531
534
537
540

Figure 4

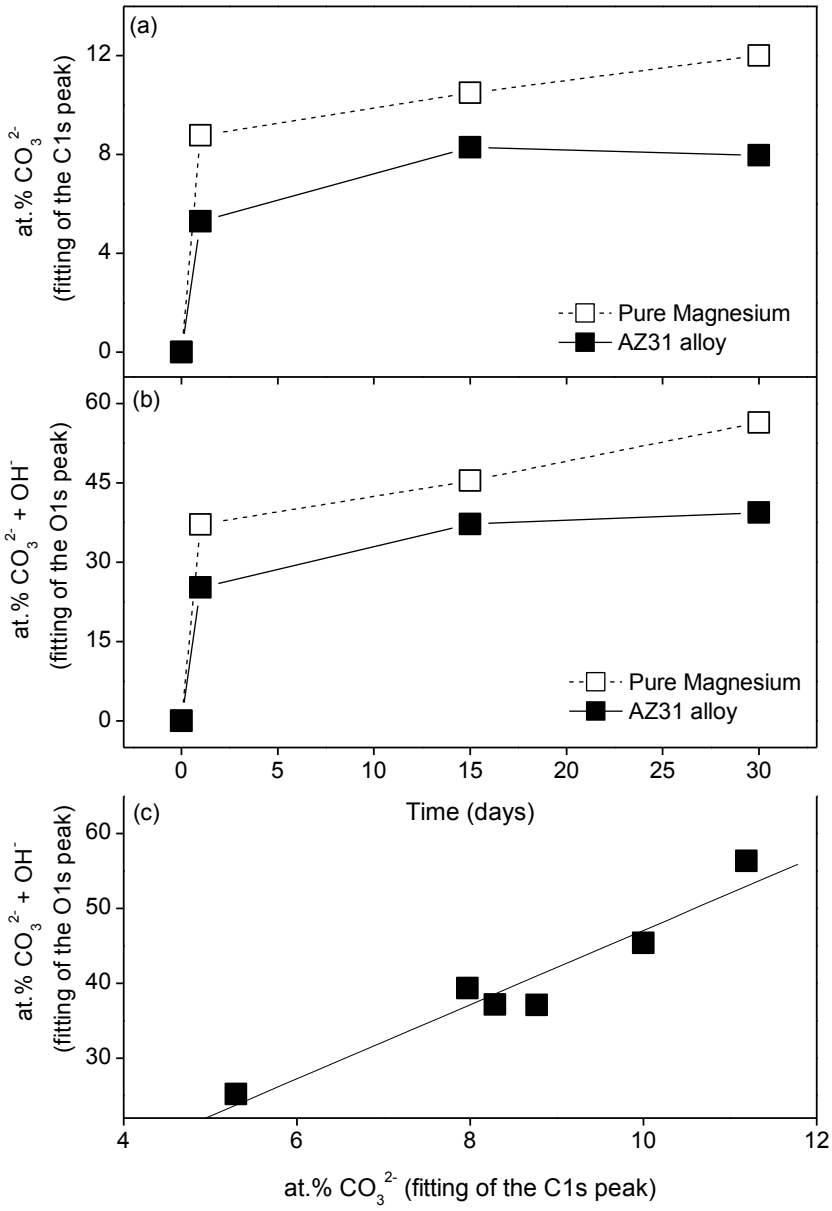
(a)
at.% CO_3^{2-} (fitting of the C1s peak)
Pure Magnesium
AZ31 alloy
(b)
at.% CO_3^{2-} + OH^- (fitting of the O1s peak)
Time (days)
(c)
at.% CO_3^{2-} + OH^- (fitting of the O1s peak)
at.% CO_3^{2-} (fitting of the C1s peak)

Figure 5

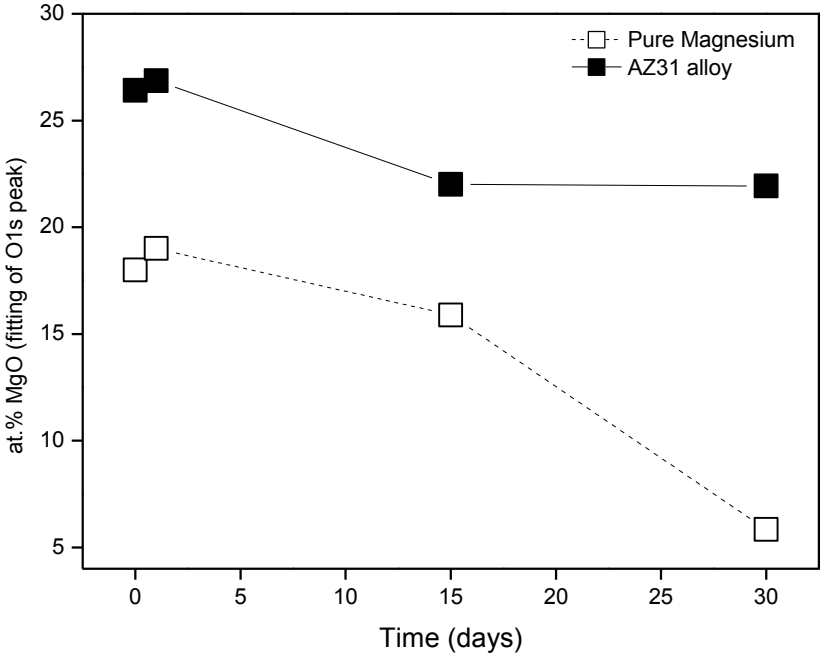
Pure Magnesium
AZ31 alloy
at.% MgO (fitting of O1s peak)
Time (days)
30
25
20
15
10
5
0
5
10
15
20
25
30

Figure 6

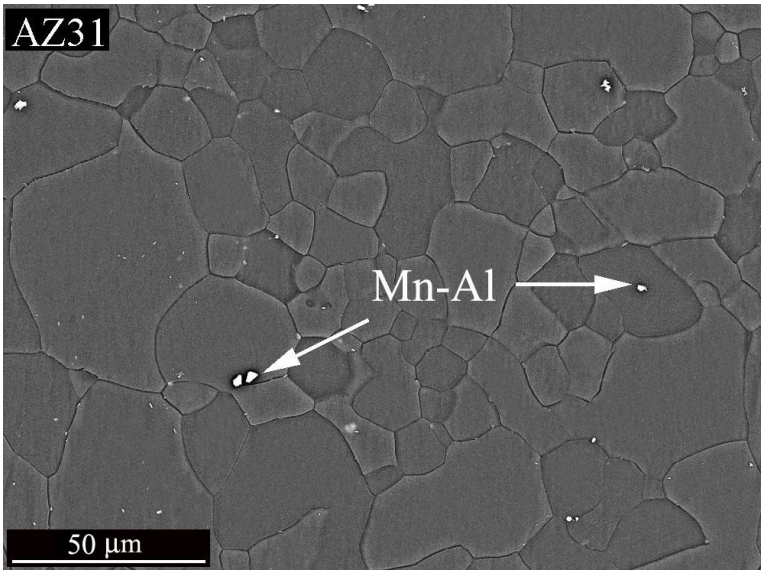

Figure 7

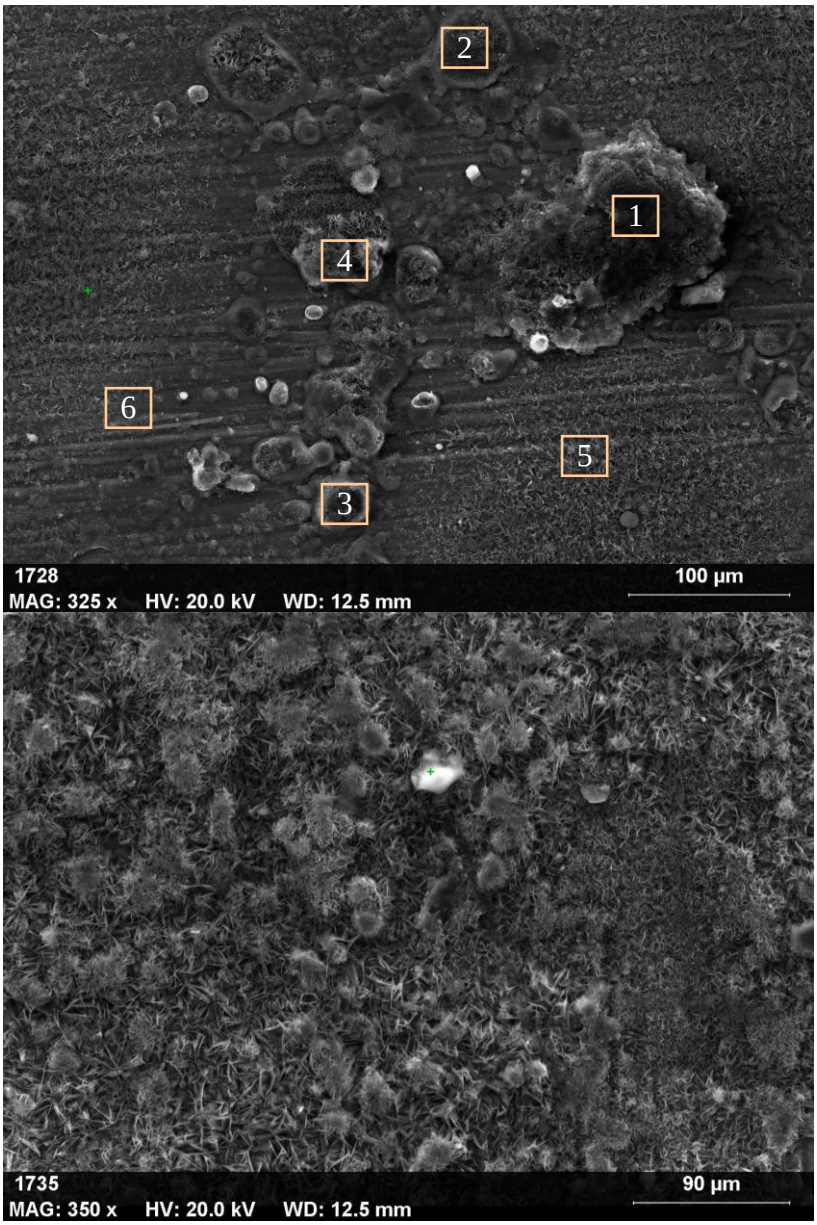
2
1
4
6
5
3
1728
MAG: 325 x HV: 20.0 kV WD: 12.5 mm
100 µm
1735
MAG: 350 x HV: 20.0 kV WD: 12.5 mm
90 µm

Figure 8